PROCEEDINGS OF SPIE

SPIEDigitalLibrary.org/conference-proceedings-of-spie

Phase correction at millimeter wavelengths using observations of water vapor at 22 GHz

Marvel, Kevin, Woody, David

Kevin B. Marvel, David P. Woody, "Phase correction at millimeter wavelengths using observations of water vapor at 22 GHz," Proc. SPIE 3357, Advanced Technology MMW, Radio, and Terahertz Telescopes, (31 July 1998); doi: 10.1117/12.317378

SPIE.

Event: Astronomical Telescopes and Instrumentation, 1998, Kona, HI, United States

Phase correction at millimeter wavelengths using observations of water vapor at 22 GHz

Kevin B. Marvel* and David P. Woody†

California Institute of Technology, Owens Valley Radio Observatory,
100 Leighton Lane, Big Pine, California, 93513

ABSTRACT

We present results from phase correction efforts at the Owens Valley Radio Observatory millimeter array (OVRO). A brief description of the theory of phase correction is followed by a description of the water line monitors (WLMs) constructed and placed on each of the six antennas of the array. A summary of the current software in place is also included. We present examples of data corrected using this technique and the first image created using radiometric phase correction at OVRO. The phase correction system is undergoing further development and will soon be made available for general observing at the array. A brief discussion of application of the technique for future arrays (e.g. MMA, LSA, etc.) is included as a conclusion to this contribution.

Keywords: Radiometric phase correction, millimeter interferometry

1. INTRODUCTION

One of the fundamental difficulties encountered when observing with radio interferometers at wavelengths shorter than a few cm is the phase corruption of astronomical signals caused during passage through the Earth's atmosphere. The main cause is the presence of varying amounts of water vapor along the line-of-sight. Strong spectral lines of water vapor are spread throughout the infrared, submillimeter and into the millimeter region of the electromagnetic spectrum. Those in the far infrared contribute significantly to a variable index of refraction in the radio regime. The variability of the refractive index is the root cause of the induced phase fluctuations. Turbulent mixing and winds aloft cause an ever-varying amount of water vapor to pass over ground-based radio interferometers. The passage of the water vapor can be traced by observing one of the atmospheric water vapor transitions (e.g. at 22 GHz) and deriving a corrective factor that can be applied either during or after the observations. This contribution summarizes current radiometric phase correction (RPC) efforts underway at OVRO as well as plans for improving the technique at the array and implications for planned large millimeter array telescopes.

Current calibration techniques at millimeter wavelengths are designed to compensate for slow instrumental or atmospheric phase drifts. Typically, short observations of a phase calibrator (e.g. strong point-like source) are interleaved with longer observations of the source of interest. In the millimeter and shorter wavelength regimes slow phase calibration cannot correct for the observed changes in interferometer phase that occur on time scales shorter than twice the calibrator cycle time. Fast phase switching improves the situation by decreasing the cycle time, but increases wear on the instrument. A renewed interest in correcting these fluctuations using radiometric techniques has been shown in recent years. Several groups (IRAM, BIMA) have attempted to use the same receivers used for astronomical observations[1,2] to determine the path-delay induced by water vapor. Our work at OVRO uses a multi-channel, water line monitor mounted at each telescope to measure fluctuations in the water vapor along the line-of-sight. We can use the WLMs to correct the interferometer phase for short term phase

* K.B.M. (correspondence): Email: kbm@ovro.caltech.edu; WWW: http://www.ovro.caltech.edu/~kbm; Telephone: 760-938-2075x105; FAX: 760-938-2075 (auto fax detect)
† D.P.W.: Email: dpw@ovro.caltech.edu; Telephone: 760-938-2075x111; FAX: as per K.B.M.

Part of the SPIE Conference on Advanced Technology MMW, Radio, and Terahertz Telescopes
Kona, Hawaii • March 1998 SPIE Vol. 3357 • 0277-786X/98/$10.00

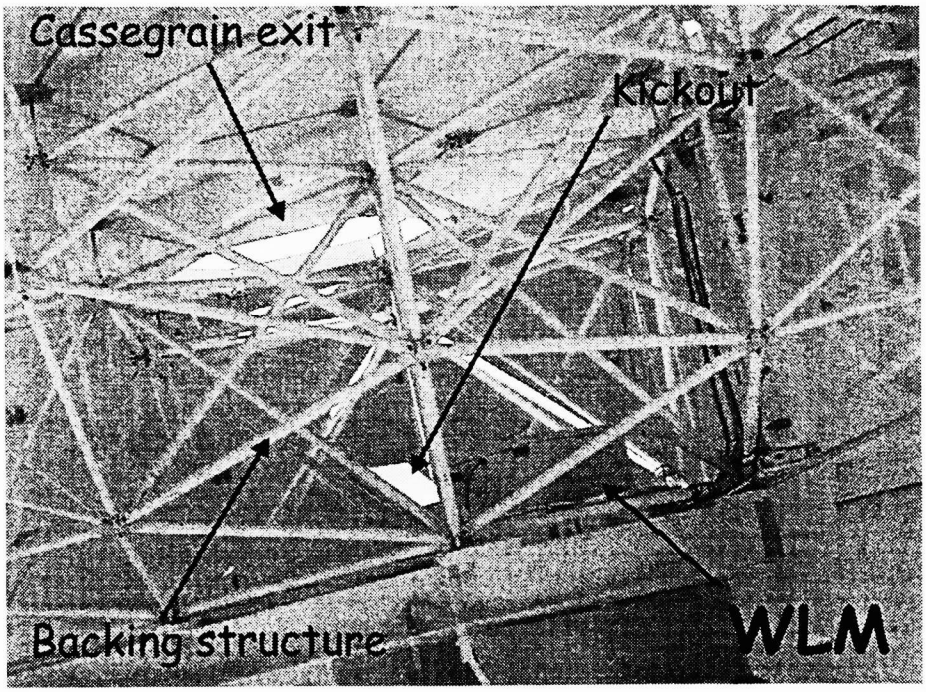

Figure 1: A water line monitor in place in the backing structure of one of the OVRO 10-m dishes. Note the kick out mirror located to the left of the WLM box.

fluctuations on time scales shorter than the cycle time. A number of theoretical papers[3,4,5,6,7] have outlined the fundamental physics involved and we present only a brief summary.

2. THEORY OF WATER VAPOR RADIOMETRIC PHASE CORRECTION

Water vapor is distributed throughout the Earth's atmosphere with a typical scale height of two km. Wind flows, convection and interactions of winds with terrestrial obstacles constantly redistribute the water vapor in a turbulent way. This turbulence causes temporal fluctuations in the water vapor content along any given line-of-sight. These fluctuations produce an ever-changing index of refraction and hence path-delay when observing in the millimeter and submillimeter regimes. The model adopted is described thoroughly in recent work[3,4,5,7]. The model assumes that the geometrical optics approximation is valid over the scale of the array and that the turbulent distribution of water vapor can be regarded as a Kolmogorov turbulent field passing over the array. The screen is assumed to be of finite thickness, which is likely a good approximation during the standard observing season at OVRO (Fall to Spring) when convection is at a minimum. We also assume that the phase delay is dominated by the water vapor, although other atmospheric constituents could play a role[7].

Under these assumptions, it is possible to write[5] the path-delay in terms of fundamental parameters. The absorption coefficient of water at a given frequency, ν, can be written as

$$\alpha(\nu) = \frac{8\pi^3}{3hc}\nu \sum \frac{\mu^2 g_i S_i}{Q} n_{H_2O}(e^{-E_{li}/kT} - e^{-E_{ui}/kT})\phi(\nu, \nu_{0i}, \gamma_i). \quad (1)$$

Here, we sum over all lines, i, having line strengths S, resonant frequencies ν_0, spin degeneracies g, and upper and lower energy states, E_u and E_l. Further, μ is the permanent dipole moment for water, n is the number density of water molecules and the remaining constants have their normal value assignments. The kinetic line shape is included as $\phi(\nu, \nu_{0i}, \gamma_i)$ and is described elsewhere[5]. If the molecular levels are populated according to the Boltzmann distribution at a given temperature T, then the partition function Q is well-behaved and has been tabulated[8]. This absorption coefficient can be integrated over a short atmospheric path, l, to give an opacity

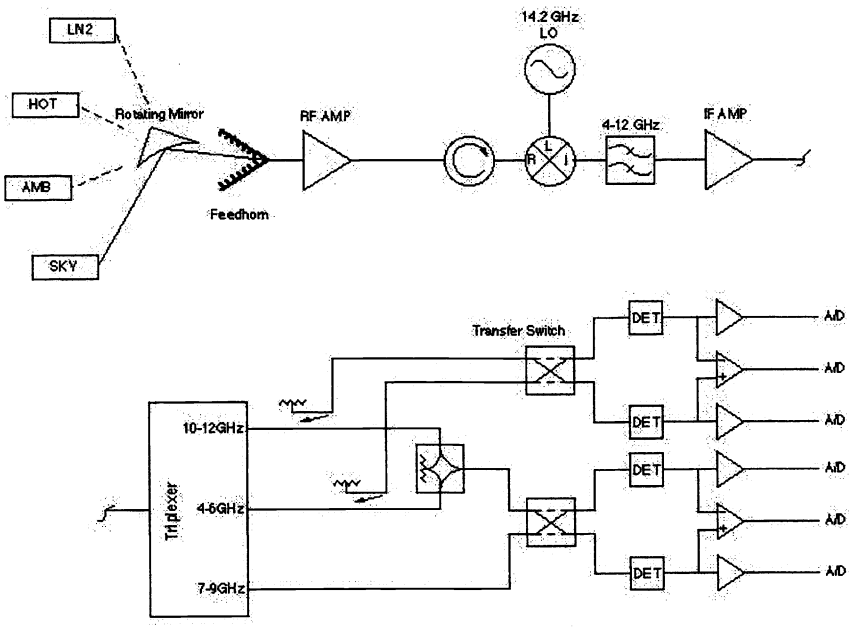

Figure 2: The block diagram of the WLM receiver system. Note the ambient, hot and sky loads, which are discussed in the text.

$$\tau(\nu) = \frac{8\pi^3}{3hc}\nu \sum_i \frac{\mu^2 g_i S_i}{Q} \rho_w w \frac{N_A}{m_{H_2O}} (e^{-E_{li}/kT} - e^{-E_{ui}/kT})\, \phi(\nu, \nu_{0i}, \gamma_i). \tag{2}$$

Here w is the precipitable water vapor content along the path of interest and is defined as

$$w = \frac{1}{\rho_w} \rho_v l. \tag{3}$$

Where ρ_w is the mass density of liquid water, ρ_v is the mass density of water in vapor form, N_A is Avogadro's number and m is the atomic mass of water. The absorption spectrum and the phase delay introduced by the water vapor are related by the Kramers-Kronig transform. Applying the transform, the path-delay can be expressed in terms of the transformed absorption spectrum:

$$l(\nu) = \frac{8\pi^2}{6hc} \sum_i \frac{\mu^2 g_i S_i}{Q} \rho_w w \frac{N_A}{m_{H_2O}} (e^{-E_{li}/kT} - e^{-E_{ui}/kT}) \frac{c}{2} \phi_{KK}(\nu, \nu_{0i}, \gamma_i). \tag{4}$$

Here ϕ_{KK} is the Kramers-Kronig transform of the line shape,ϕ. The opacity at the frequency of interest depends on all of water vapor line strengths, shapes and degeneracies but is dominated by those in the far infrared. For the purposes of phase correction, this derivation is enough to proceed as a change in the water vapor content along our line of sight is now related to the path-delay. It has been shown[5,7] that in the millimeter regime the relationship between the precipitable water vapor content and delay is nearly linear as a function of frequency. We have only to measure the varying amount of precipitable water vapor to derive the induced path-delay and need not determine the exact opacity as given in equation 2.

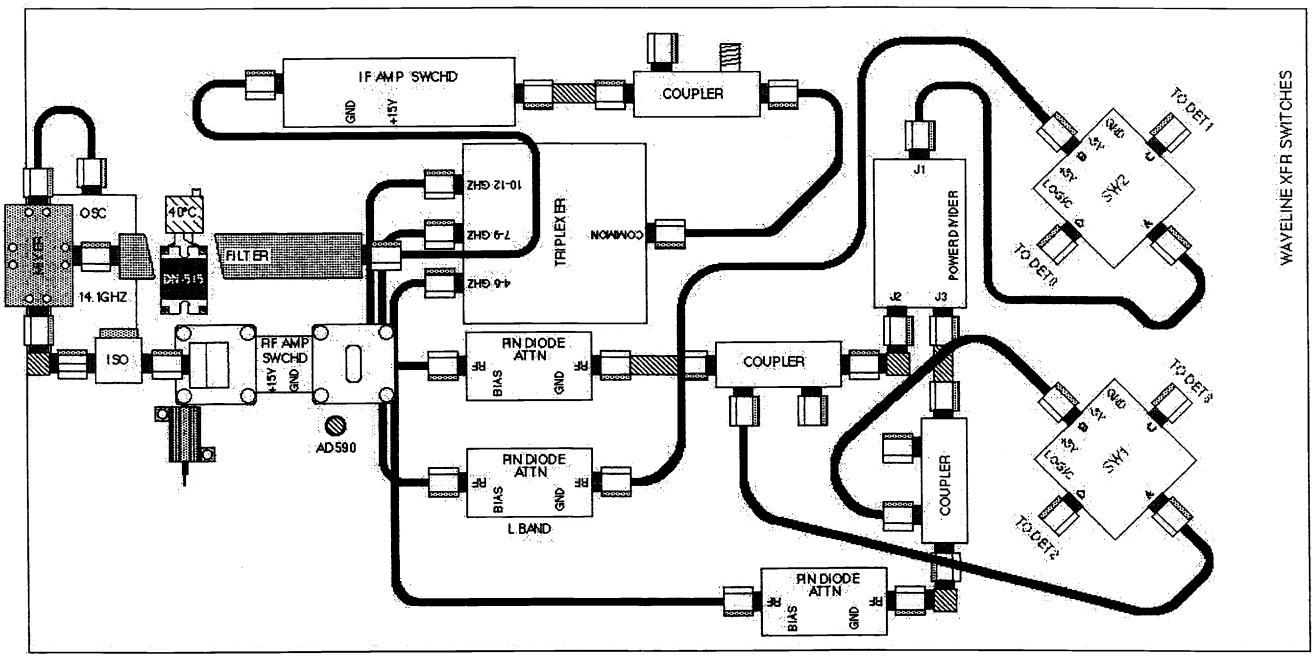

Figure 3: The RF plate layout for the WLM.

Some variation with temperature and pressure are expected but they do not significantly affect the linear relationship in the millimeter regime.

The atmospheric opacity near the 22 GHz water line can be broken into three dominant components[5]:

$$\tau_{H_2O} = A_\nu \, w_o + B_\nu + A_\nu \, w_{\mathrm{var}}. \tag{5}$$

The three constituents (from left to right) are the non-variable opacity contribution from water vapor, opacity sources from other atmospheric constituents (including liquid water) and the time variable water vapor contribution. The *A* terms are the opacity contribution per mm of precipitable water vapor as a function of frequency. By writing the opacity in this form, we may isolate the term of interest, namely the time variable component, $A_\nu \, w_{var}$. This component causes a time-variable atmospheric brightness temperature which can be derived[5] using the radiometry equation[9] and the opacity as written in equation 5. To good approximation the ***time-variable*** brightness temperature due to fluctuation of water vapor content as a function of frequency is given by:

$$T_b(\nu) = T_{atm} e^{-\tau_0} A_\nu w \, . \tag{6}$$

Where τ_0 is assumed to be a mean optical depth with the form[7], $A_\nu w_\nu + B_\nu$. It becomes very difficult to solve for the WLM gains described in the next paragraph in the limit of very low water vapor column densities. However, under these conditions, corrections to the phase may not be required to obtain excellent data.

In principle, we measure the temporal changes in the 22 GHz water vapor line contrast with the three channels of the WLM (two continuum channels, one line-center channel). The path delay is linearly related to the water vapor column, which is related to the observed line brightness. The difference in the path delay is proportional to the observed interferometer phase. We use phase measurements of a strong point-like source (known phase) to derive the exact constants of proportionality, G_i (as shown in the following equation)

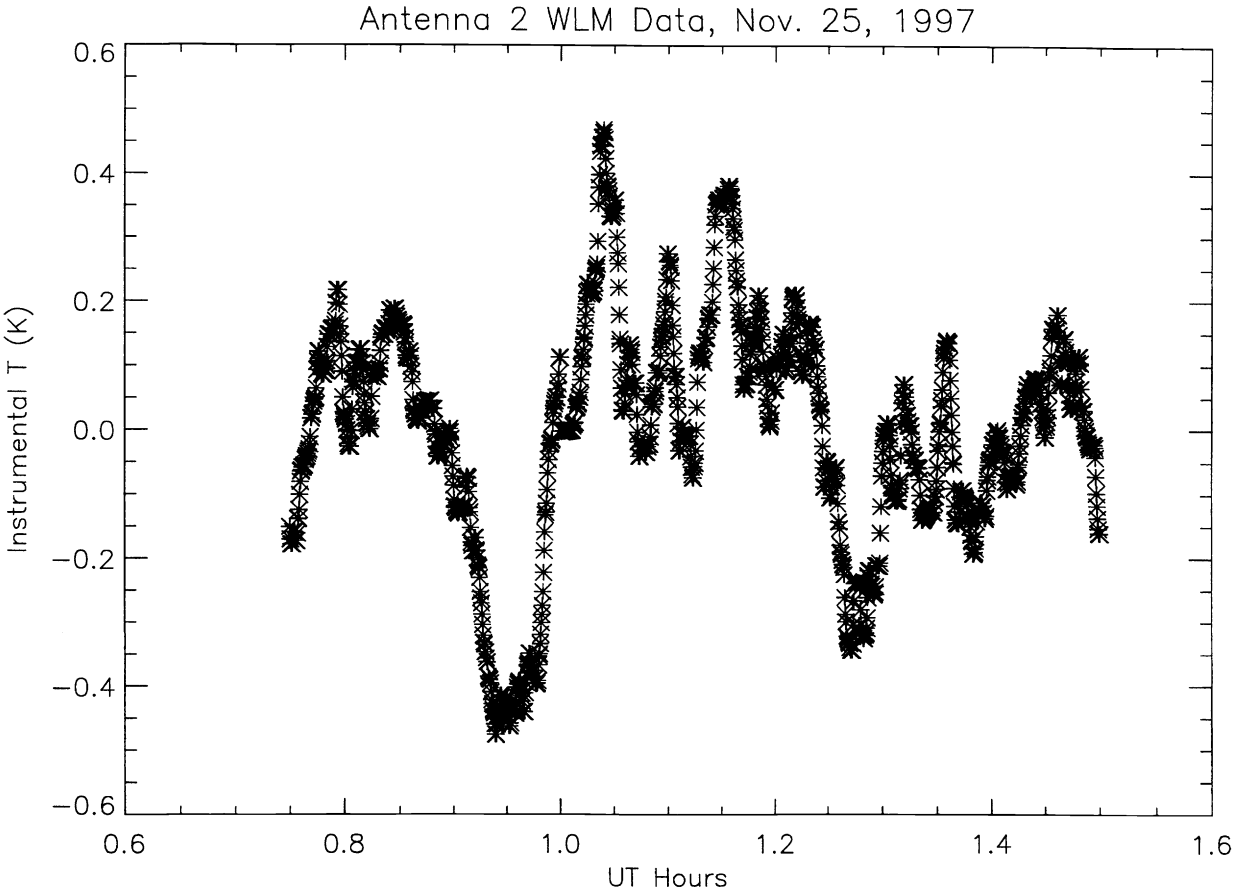

Figure 4: Time series of measurements from a single WLM. The time spanned is approximately one hour. Note the variability of the data over short times. The vertical axis is relative to the mean instrumental T.

$$\phi_{i-j}(t) = G_i T_i(t) - G_j T_j(t). \tag{7}$$

Here we show the relationship between the observed baseline phase (expressed as a delay) and the fluctuations in the line contrast. The G_i terms convert the measured line contrast to delay. In the current exploratory mode, the software performs a baseline-to-baseline fit. In the next software version currently under development a generalized singular value decomposition solution will be made for the G_i terms.

3. RPC HARDWARE IN OPERATION AT THE OVRO MILLIMETER ARRAY

The design goal for the WLMs was to determine the path delay to an accuracy of .05 mm on time scales from 1 sec to 1 hour during typical observing conditions. It was decided to measure the 22.2 GHz water vapor line using standard commercial components all operating at room temperature. The 22.2 GHz line was picked because it is not saturated at the 4,000-ft elevation of OVRO and reasonably priced commercial components are available in this frequency range. The sensitivity, stability, and continuum rejection are the critical performance parameters.

A WLM mounted on one of the OVRO 10-m dishes is shown in Figure 1. Figure 2 shows a block diagram of the WLM and the component layout is shown in Figure 3. The front-end amplifier is a commercial 18-26 GHz amplifier with a 2-dB noise figure. The output from this amplifier is down converted into the 4-12 GHz where commercial components are less

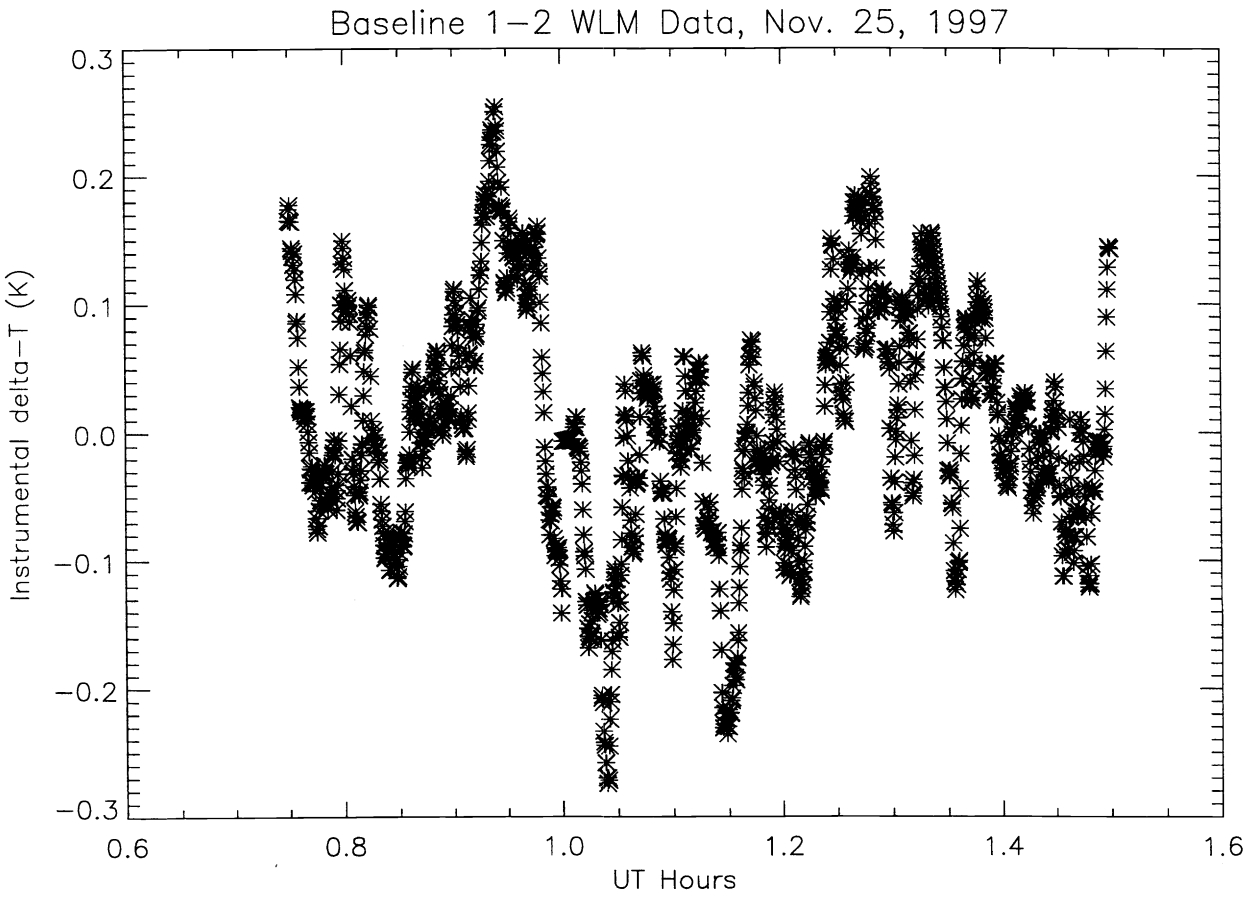

Figure 5: The time series of WLM data for a given baseline. The time spanned is approximately one hour. The data points are separated by approximately 2 s.

expensive. This broadband signal is amplified and divided into three 2 GHz wide channels by a triplexer. The two continuum channels, C1 and C2, are centered at 3 GHz above and below the 22.2 GHz line while the line channel, L, is centered on the line itself. The two continuum bands are summed to form a single continuum band, C. The L and C bands feed a transfer switch with the output going to two detectors. The output from the detectors is amplified and boxcar integrated and measured by a 16-bit A/D in a PC computer running LABVIEW under a Windows NT operating system. The analog difference between the output from the two detectors is amplified by an additional factor of ten before integrating and sampling. This analog difference channel provides the fundamental data for determining the water vapor line emission. Another transfer switch and pair of detectors also monitors the C1 and C2 bands. These bands will be used for determination of the continuum slope and identification of the magnitude and source of the continuum emission.

The relatively large bandwidth for the individual channels was dictated by the requirement to achieve .05 mm delay sensitivity in only one second. The nominal conversion factor from line temperature to delay is 6 mm/K, i.e. the radiometry sensitivity needs to be .01 K/$\sqrt{\text{Hz}}$. This can be accomplished with a 200 K noise temperature and a 2 GHz bandwidth.

The WLMs are designed to maximize the sensitivity to the 22.2 GHz water vapor line while rejecting sources of continuum emission. Rejection of continuum emission is particularly important for successful operation during normal observing conditions. Thin or partial cloud cover can exist while having low receiver noise temperatures and reasonable phase stability. The ratio of opacity to index of refraction for liquid water is nearly a factor of 50 larger than it is for water vapor. Therefore the fluctuations in the liquid content in clouds can dominate the continuum brightness fluctuations and disrupt any attempts to determine the path-delay variations due to water vapor. There are other sources of continuum emission , such as spillover,

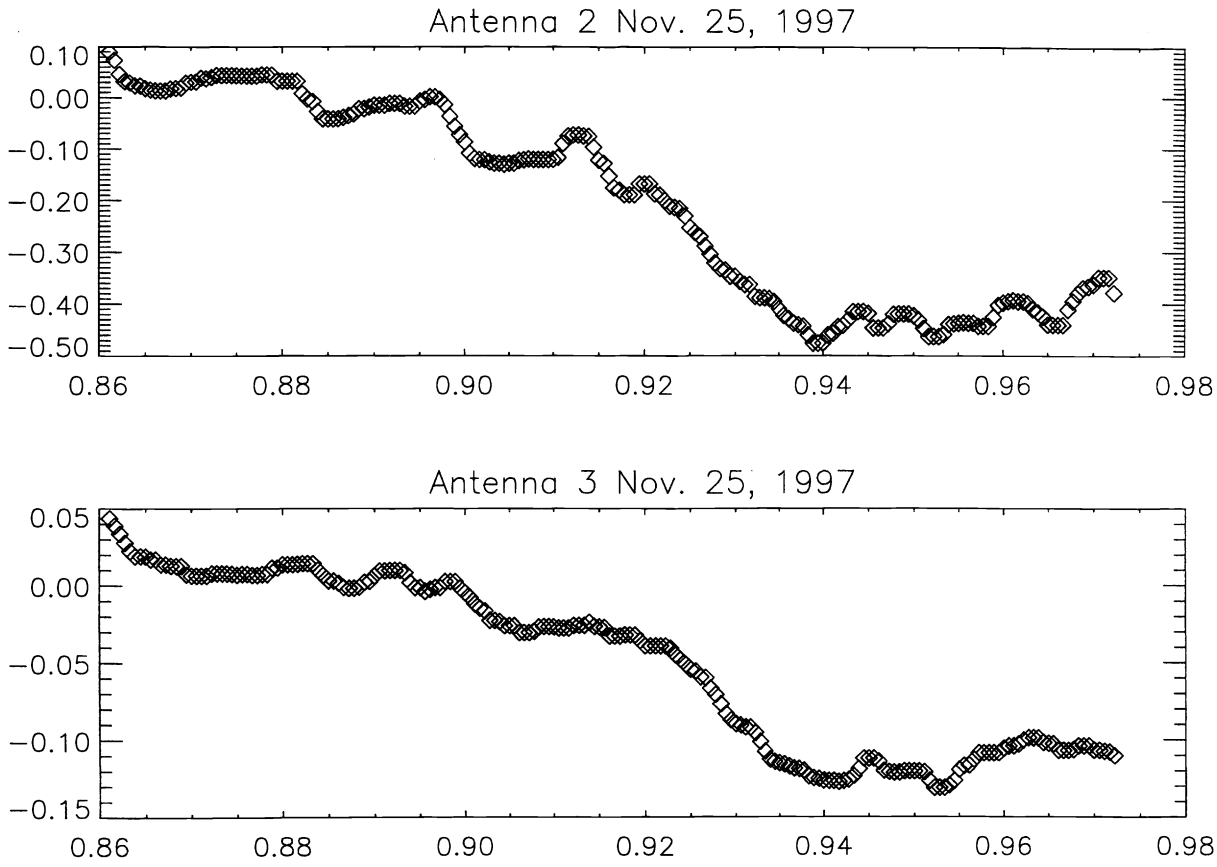

Figure 6: Time series WLM data for two telescopes. The baseline is 150m long and oriented E-W. The derived lag using the cross-correlation technique described in the text is approximately 4s. The derived pattern direction is SW-NE.

that can also interfere with path-delay determination. The laboratory measurements indicate that the L-C response rejects blackbody continuum emission by more than a factor of 100.

Long-term changes require minimizing all sources of drift. Using a common amplifier for the three channels removes the effect of flat gain chains. The transfer switches are reversed after every 2 msec box-car integration time. This removes most of the detector gain and offset drifts. The most significant drift left is the second order change in the gain as a function of frequency for the RF and IF amplifiers.

The WLMs are calibrated using thermal loads at ambient temperature and 90° C. These loads are triangular troughs with an emissivity estimated to be greater than 99.9%. Their temperatures are measured with a precision of .01 K. The absolute gain and the system noise temperature for the three channels are determined using the standard hot/cold Y-factor technique. Typically this calibration takes ~5 sec and is performed every 20 min. Several times during the observing season, the WLMs are checked for linearity and gain equalization. The linearity is measured using a liquid nitrogen load in addition to the ambient and 90° C loads. The gain equalization is adjusted using the pin-diode attenuators for the three channels. They are adjusted to give equal gains for the three channels. This results in zero change in output from the analog differences L-C and C1-C2 for the set of thermal loads. Laboratory measurements indicate that the gains are stable enough to link the phases of nearby calibrators but this remains to be verified for operation on the telescopes.

Six WLMs have been built and installed on the Leighton telescopes in the OVRO millimeter interferometer array. They are located in the backing structure as shown in Figure 1, and look at the secondary via an off axis ellipsoidal mirror (kickout).

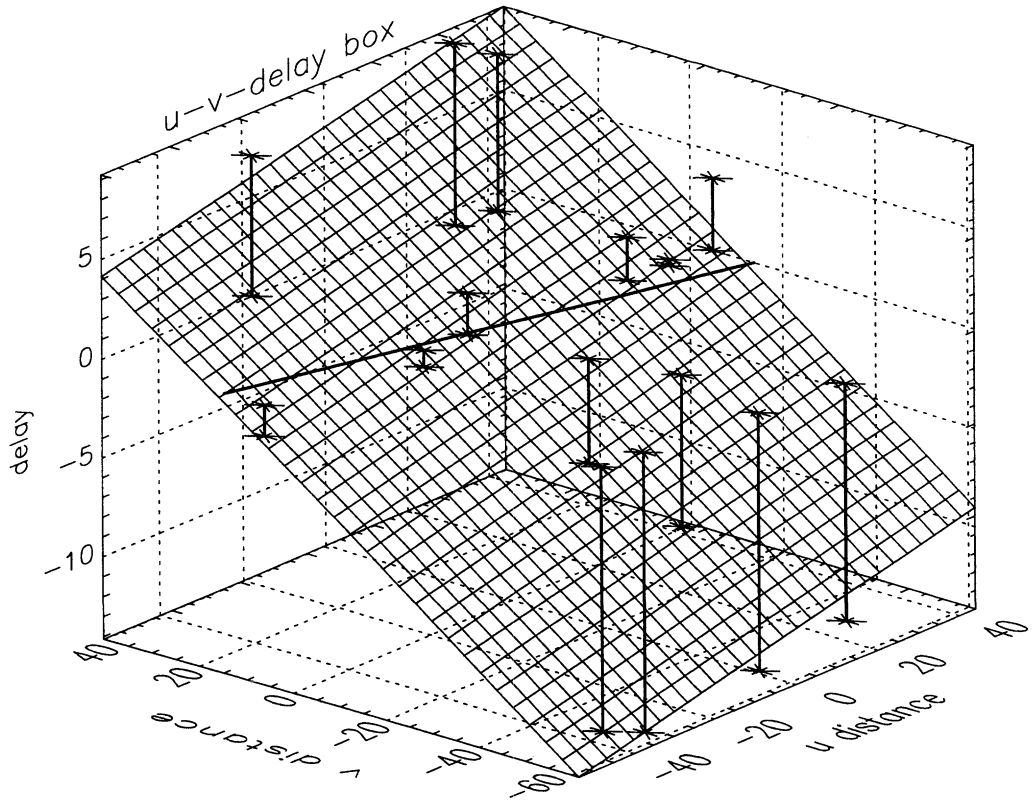

Figure 7: The result of the delay analysis discussed in Section 5. The vertical axis is delay in seconds derived from a time-series cross-correlation analysis. The horizontal plane is the u,v plane. The vertical lines plotted begin at the delay = 0 plane and end at the location of a single calculated delay. The plane segment plotted is the result from fitting a plane to the indicated data points. The horizontal line crossing the diagram is the intersection line of the delay = 0 plane and the fitted wind pattern plane. The gradient of the plane, rotated to array coordinates, indicates the water vapor pattern speed and direction.

This mirror is positioned to not interfere with the millimeter receiver beams but still produce a beam on the sky that is only 10 arcmin from the astronomical beam. The astronomy beam and the WLM beam traverse the same 10 m diameter air column in the near field. The beams diverge by ~10 m at a distance of ~4 km. This insures that most of the water vapor in the atmosphere is seen in common.

4. RPC SOFTWARE IN OPERATION AT THE OVRO MILLIMETER ARRAY

The control software for the WLMs has been implemented in a commercially available graphical programming environment, LABVIEW, produced by National Instruments of Austin, Texas. Each of the six telescopes is equipped with a Pentium-class computer, which runs the real-time data acquisition software. These computers are networked to a central server, which serves as a central repository for the source code, facilitating upgrades and backups, as well as performing as a timeserver. Several data records are written to local hard disk every second. These include current calibration information as well as observed power in each of the three channels. The system will soon be upgraded with the addition of a database connectivity package. This package will allow direct data deposition using the Sybase database server in operation at the site.

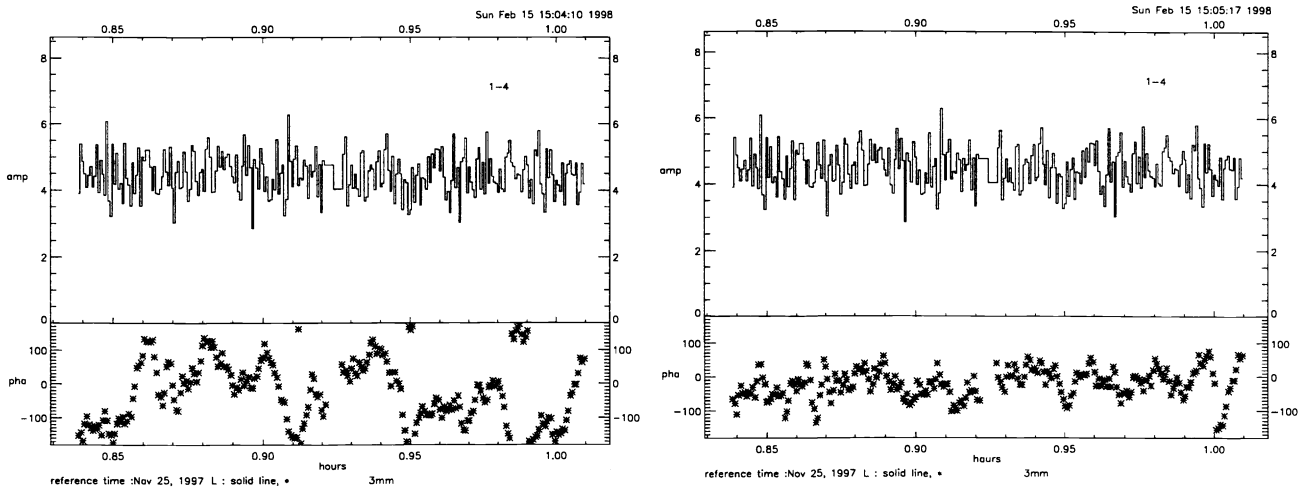

Figure 8: A comparison of two integrations of data (125 records/int) from the November 25, 1997 track on 3C454.3 for Baseline 1-4. Raw data on the left, corrected data on the right. Note the dramatic improvement in the baseline phase after application of the WLM correction. The deviation at the end of the time range is due to missing WLM data.

The data are processed using reduction software written in LABVIEW. This package coverts the raw instrumental power measurements in each of the three channels to temperature units in the water line and interpolates the data onto a common time axis. The data are then read into new reduction software under development at the array named the Millimeter Interferometer Reduction (MIR) package. MIR is written in the Interactive Data Language (IDL) and is a site-specific interferometric data reduction package. An example of one hour of water line data from a single telescope is shown as Figure 4. The baseline temperature differences are then formed. An example of a single baseline of data is shown as Figure 5.

In the current developmental phase of the correction system we have attempted to correct only for on-source phase fluctuations and not full radiometric phase correction as outlined in recent work[4]. Pending successful implementation of the on-source scheme, we will implement the full radiometric correction method.

To perform the on-source only calibrations, the relationship between observed brightness on the water vapor line and the observed phase fluctuations must be determined. This relationship is not necessarily stable with time due to a number of causes, namely time-variable receiver changes and changes in the turbulent layer(s). Once the gains are determined, the calibration can be applied, and normal phase referencing used to reference the phase on the source of interest to the phase reference source.

We perform a long observation (~30 min) of a strong point-like source to calibrate the individual antenna gains. We break the observation into five minute integrations (each containing 125 records). After converting the raw antenna-based temperatures to phase using *a priori* conversion factors determined from laboratory calibration of the WLMs, we solve for the individual WLM gains as in equation 7. We have found that a robust regression algorithm, which is insensitive to extreme points works best in determining the WLM gains.

5. WATER VAPOR PATTERN SPEED AND DIRECTION

The water vapor pattern speed and direction can be deduced from the observed time series data obtained with the WLMs. As the water vapor screen passes over the array, a signal is first detected at windward telescopes and subsequently at leeward telescopes. Forming the cross-correlation of the signals amongst all non-redundant pairings of telescopes allows a determination of the direction and speed of the water vapor pattern. An example of the time series data obtained from two widely separated antennas is shown in Figure 6. The baseline is 165 meters long and is oriented E-W. The lag between the time series data is approximately 4 seconds (as determined using the technique described below).

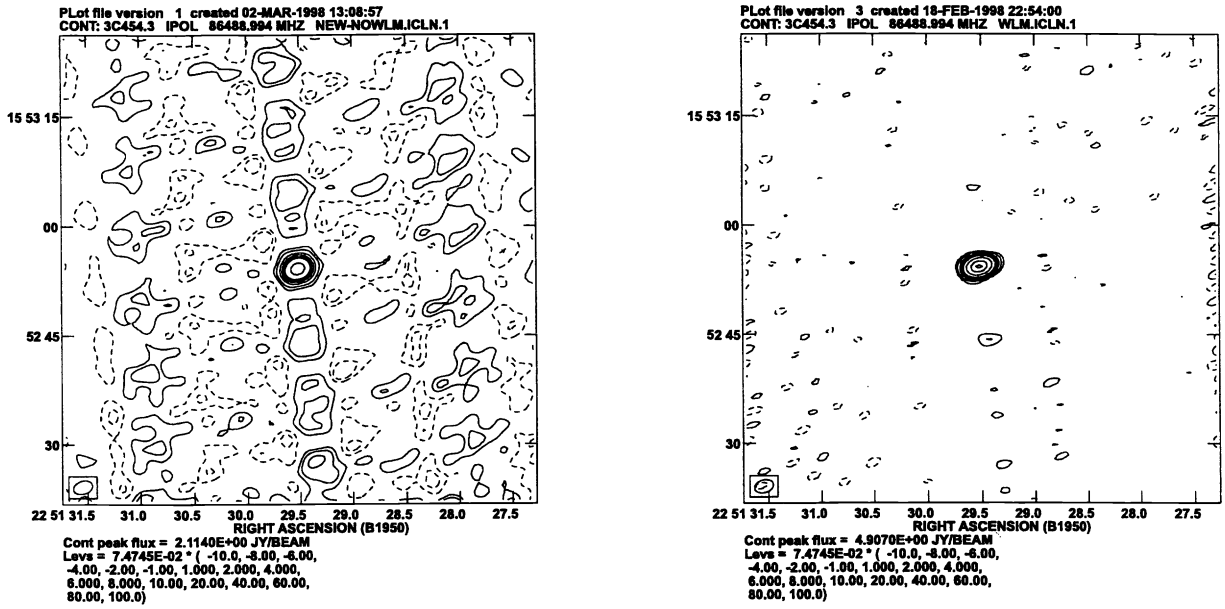

Figure 9: An example of the image quality improvement using the on-source WLM phase correction technique. The image on the left was formed from the same one-hour data set as the image on the right but without WLM correction applied. The source is 3C454.3. The two images are contoured to the same level for comparison purposes. The data forming the left-hand image would have been re-observed under better weather conditions. The remaining image artifacts in the corrected (left-hand) image are due to dynamic range limitations.

The approach we have adopted can be summarized as fitting a plane in *u-v-delay* space. Delay here should not be confused with the geometric delay. After forming the time series cross-correlation amongst all possible pairings of WLM boxes, the resultant peaks in the lag domain were fit by a Gaussian function. The offset from zero delay indicates the time lag between detection of a water vapor cloud at the two telescopes.

One can then assign a *u, v* coordinate to each delay measurement over an appropriately short length of time (~30 min). The points lie on a plane in *u-v-delay* space. After fitting a plane to the points, the water vapor pattern speed can be determined by simply rotating the gradient of the plane into array coordinate space (N, E, UP) and projecting onto the N-E plane. A plot of the fitted plane is shown as Figure 7. Note that the time resolution of the WLMs (1s) is insufficient to detect vertical motions of the water vapor pattern.

We have performed this analysis for a track obtained on November 25, 1997, and have compared the derived pattern direction and speed to the recorded ground conditions. For this date, the derived pattern speed was 17.5 m/s from a SSW direction. For the same day and time, the recorded ground speed at OVRO was 5 m/s from the SW. We have also obtained wind speed and direction measured with radiosonde at the Department of Energy Mercury test facility located near Las Vegas, Nevada approximately 150 miles away to the SE. The altitude, as measured by radiosonde, that has a measured wind speed similar to the derived pattern speed is 4100 m with a direction of 240 degrees (~WSW).

If the derived pattern speed is caused by the same winds measured at the Mercury site, then the phase fluctuations are probably caused at the shear layer between the relatively calm valley air and the fast moving high-altitude air. OVRO resides

at an altitude of approximately 1200-m, while the Sierra Nevada Mountains to the west and south have a peak altitude near 4000-m. We plan to use this technique combined with a crossed beam technique to determine the true altitude of the phase fluctuation layer. Results from this planned study could have significant impact on planned large millimeter arrays at higher altitudes.

6. PHASE CORRECTION RESULTS FROM WLM DATA

We have also successfully used the software described in Section 4 to correct a short observation of the quasar 3C454.3. The average RMS phase improves by a factor of two to three. An example of a short time-span of data on a single baseline with and without the WLM phase correction is shown as Figure 8. Normal phase calibration with a smoothing time of 20 minutes was applied to both the raw and WLM corrected datasets. Maps were then formed and are shown in Figure 9.

Prior to the phase correction, the coherence on most baselines was less than 0.3 and this track would have been classified as bad and likely re-observed under better weather conditions. With the RPC applied, the image fidelity is greatly improved and the source resides at the phase center, as it should. The dynamic range is nearly 200, close to the theoretical dynamic range limit for the array and the flux peak matches that expected. The data would be considered good.

7. CONCLUSIONS

This work has shown that radiometric phase correction can be used to dramatically improve the quality of data produced by millimeter interferometers. At the least, the technique can be used to improve the coherence on short time scales, essentially freezing the atmosphere and improving the seeing. Future development of the technique at OVRO will include testing and developing algorithms for application of the correction to higher frequencies as well as using the WLMs to provide full radiometric phase correction.

8. ACKNOWLEDGEMENTS

K.B.M. acknowledges the support of a California Institute of Technology postdoctoral fellowship during the time this work was performed.

9. REFERENCES

1. M. Bremer, S. Guilloteau and R. Lucas, "The phase project: observations of quasars", IRAM Working Report Number **238**.
2. W. J. Welch, "The Berkeley-Illinois-Maryland-Association array" ASP Conference Series Vol. 59, p. 74.
3. O. P. Lay, "The temporal power spectrum of atmospheric fluctuations due to water vapor", Astronomy & Astrophysics Supplement Series **122**, pp. 535-545.
4. O.P. Lay, "Phase calibration and water vapor radiometry for millimeter-wave arrays", Astronomy & Astrophysics Supplement Series **122**, p. 547.
5. E. C. Sutton and R. M. Hueckstaedt, "Radiometric monitoring of atmospheric water vapor as it pertains to phase correction in millimeter interferometry", Astronomy & Astrophysics Supplement Series **119**, pp. 559-567.
6. M. Bremer, "Phase monitoring with cloud correction near the 22.2 GHz water line", IRAM Working Report Number **247**.
7. C. L. Carilli, O. Lay, E. C. Sutton, "Radiometric phase correction", VLA Scientific Memo Number
8. R. L. Poynter and H. M. Pickett, "Submillimeter, millimeter and microwave spectral line catalog", JPL Publication 80-23, Revision 2.
9. R. H. Dicke, R. Beringer, R. L. Kyhl, and A.B. Vane, Physical Review, Vol. 70, p. 340.